An Si–SiGe BiCMOS Direct-Conversion Mixer With Second-Order and Third-Order Nonlinearity Cancellation for WCDMA Applications

Liwei Sheng and Lawrence E. Larson, *Fellow, IEEE*

***Abstract*—This paper presents a general analysis of the third-order nonlinearity of a differential common-emitter RF amplifier and an improved technique to cancel the third-order nonlinearity. A thorough analysis of the mechanisms leading to the second-order nonlinearity of bipolar double-balanced active mixers is also presented. An SiGe BiCMOS WCDMA direct-conversion mixer is designed based on the third- and the second-order cancellation schemes. The mixer achieves +6-dBm third-order input intercept point, +49-dBm second-order input intercept point, 16-dB gain and 7.2-dB double-sideband noise figure with only 2.2-mA current at 2.1 GHz.**

***Index Terms*—Active mixer, BiCMOS, direct conversion, mismatch, nonlinearity cancellation, radio receivers, second-order distortion, second-order input intercept point (IIP2), Si–SiGe analog integrated circuit (IC), third-order distortion, third-order input intercept point (IIP3), WCDMA.**

I. Introduction

LOW-POWER, high-performance, and low-cost integrated RF circuits are aiding the rapid growth of mobile wireless communications. The bipolar common-emitter (CE) and differential-pair stages are commonly used in many RF building blocks such as low-noise amplifiers (LNAs) and mixers. Fig. 1 is the block diagram of a direct-conversion receiver. For a direct-conversion WCDMA system, the linearity requirements of the mixer are greater than 0-dBm IIP_3 and 35-dBm IIP_2 if the LNA preceding the mixer has a gain of approximately 16 dB and a surface acoustic wave (SAW) filter is placed in between the LNA and mixer [1]. The inherent linearity of a CE circuit does not satisfy these requirements unless the dc power dissipation is very high. Inductive or resistive degeneration is usually applied to improve the linearity of these circuits, though it sacrifices the gain or raises dc current [2]. Another way to improve the linearity is to utilize the second-order nonlinearity to cancel the third-order nonlinearity [3]. This method achieves high linearity at lower bias current, but requires a complicated nonlinear analysis. Recently, several authors [3]–[5] analyzed the problem and showed that up to 14-dB linearity improvement can be achieved with proper choice of source harmonic termination.

In Section II, we directly compute the nonlinear response of a differential CE circuit. The direct nonlinear response is solved, then a relatively straightforward expression for third-order nonlinearity cancellation is given.

The use of direct-conversion techniques is a promising approach for highly integrated wireless receivers due to their potential for low-power fully monolithic operation and extremely broad bandwidth [6]. Their potential for broad-band operation is especially important for future wireless communication applications, where a combination of digital cellular, global positioning system (GPS), and wireless local area network (WLAN) applications are required in a single portable device. However, it also exhibits some disadvantages compared to a heterodyne receiver [7]. One limiting factor is the envelope distortion due to even-order nonlinearities. If a direct-conversion receiver architecture is used, a second-order input intercept point (IIP2) performance as high as 70 dBm is required in many RF systems [8]. Several recent papers have focused on the cancellation of the even harmonic distortion in direct conversion receivers [8]–[12]. In [8], even-order distortion is modulated to the chopping frequency through dynamic matching without trimming the mismatching devices. It provides an IIP2 improvement of approximately 16 dB with a risk of undesirable spurious response. The behavioral models of even-order distortion for single- and double-balanced mixers are given in [10]. Although a simplified switching model was used for the single-balanced mixer model, the IIP2 performance improvement of approximately 25 dB was achieved for the single-balanced mixer [10]–[12]. In the double-balanced behavioral model, an "equal gate" function was assumed for two pairs of switching transistors [10]. If the two pairs of switching transistors are mismatched, the "gate" functions are not equal. Thus, the capability for even-order distortion cancellation by tuning the load resistance in a double-balanced mixer is impaired. A more detailed analysis is required to account for the effects of mismatches on switching transistors on the double-balanced mixer. In Section III, an even-order distortion model with consideration of the β mismatch, the saturation current mismatch, and the bias voltage mismatch of the double-balanced mixer is provided and an even-order distortion cancellation technique is given.

Manuscript received April 17, 2003; revised June 28, 2003. This work was supported by the Center for Wireless Communications, University of California at San Diego, and its member companies, by the University of California Discovery Grant Program, and by IBM under the University Partnership Program.

The authors are with the Department of Electrical and Computer Engineering, University of California at San Diego, La Jolla, CA 92037 USA.

Digital Object Identifier 10.1109/TMTT.2003.818586

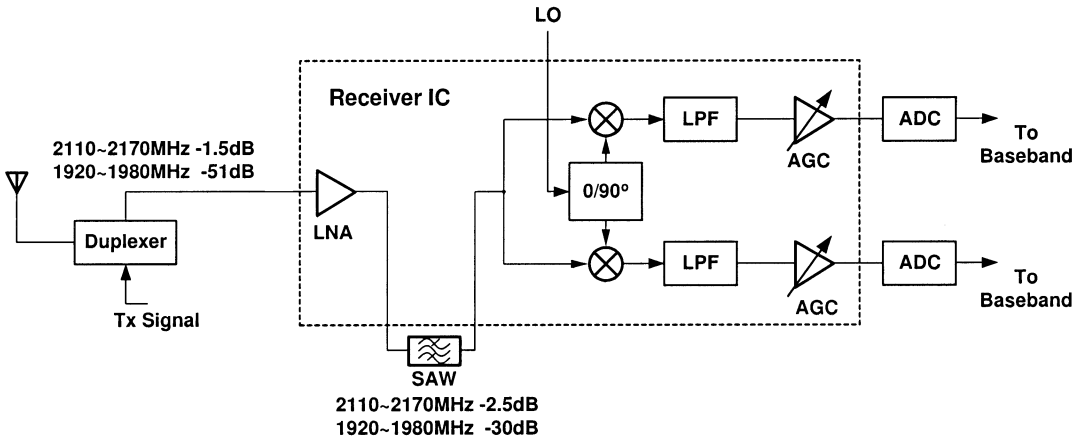

Fig. 1. Simplified block diagram of a direct-conversion WCDMA receiver.

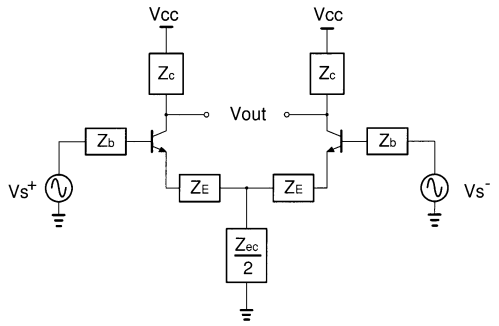

Fig. 2. Large-signal model of a CE differential pair.

II. Odd-Order Nonlinearity Analysis of a Differential CE Circuit

Fig. 2 shows the model used for analysis on the nonlinearity of the differential CE circuit. Z_b is the impedance at the bases of the transistors, which includes the impedance of the bias network, base resistance, source impedance, and impedance of the matching network. Z_c is the impedance at the collector of the transistor, which includes the impedance of the collector–substrate capacitance $C_{\rm cs}$, the collector resistance r_c, and the load impedance. Z_{ed} includes the extrinsic emitter resistance r_e and outside emitter termination impedance Z_E. $Z_{ec}/2$ is the impedance from ground to the connecting point of the two emitters.

To simplify the analysis, the following assumptions were made, similar to that in [3]. The collector current is only a function of the base–emitter voltage. The Early effect is ignored because the transistor output resistance is much larger than the output load for RF applications. For mixers, the output load is the impedance of the emitters of the upper switching pairs, which is close to the input impedance of a common-base circuit. The base–emitter junction capacitance C_{je} is considered as a linear component because its nonlinearity is small compared to the base–emitter diffusion capacitance $C_{\rm DE}$. The base resistance r_b, extrinsic emitter resistance r_e, base–collector capacitance C_μ, collector–substrate capacitance $C_{\rm CS}$, forward transit time τ, and the low-frequency current gain β are all constant because their nonlinearities are small compared to the nonlinearity of the g_m.

The nonlinear components are collector current i_c, base current i_b, and base–emitter diffusion capacitance current $i_{C_{\rm DE}}$. They are all functions of base–emitter voltage $v_{\rm be}$, i.e.,

$$i_c = g_m v_{\rm be} + g_{m2} v_{\rm be}^2 + g_{m3} v_{\rm be}^3 \tag{1a}$$

$$i_b = \frac{i_c}{\beta} \tag{1b}$$

$$i_{C_{\rm DE}} = \tau \frac{d}{dt} i_c \tag{1c}$$

where $g_m = I_{c0}/V_t$, $g_{m2} = I_{c0}/2V_t^2$, $g_{m3} = I_{c0}/6V_t^3$, I_{c0} is the dc collector current, β is the dc current gain, τ is the forward base–emitter transit time, and $V_t = kT/q$.

The first-order response is given by

$$V_{\rm out1} = H_d(s) V_s \tag{2}$$

where

$$\begin{aligned} V_s &= V_s^+ - V_s^- \\ H_d(s) &= \frac{Z_c\left\{C_\mu s\left[1 + (g_m + C_\pi s) Z_{ed}\right] - g_m\right\}}{L_d(s)} \\ C_\pi &= C_{je} + \tau g_m \\ Z_{ed} &= r_e + Z_E \\ L_d(s) &\cong 1 + g_m\left(Z_{ed} + \frac{Z_b}{\beta}\right) + C_\pi s(Z_b + Z_{ed}) \\ &\quad + C_\mu s\left(Z_b + Z_c + (g_m + C_\pi s)\Delta_d\right) \end{aligned}$$

and

$$\Delta_d = Z_{ed} Z_b + Z_b Z_c + Z_{ed} Z_c.$$

The third-order currents are generated in two ways: through the third-order transistor transconductance g_{m3} and the interaction of first-order response and the second-order response through second-order transconductance g_{m2}. Solving the third-order solution through the use of a Volterra series [13], we have

$$V_{\rm out3} = g_{m3} \cdot G_d(s)_3 \left\{ K_d(s) V_s \cdot \left[F_d(s)_2 \left(\frac{K_d(s) V_s}{2} \right)^2 \right] \right\} \tag{3}$$

where

$$F_d(s) = \frac{1}{L_c(s)} \times \left\{1-2g_mZ'_e-2g_m\frac{Z_b}{\beta}+(C_{je}-2\tau g_m)s(Z_b+Z'_e) +C_\mu s\left[(Z_b+Z_c)(1-2g_mZ'_e) +\Delta_c(C_{je}-2g_m\tau)s-2g_mZ_bZ_c\right]\right\}$$

$$G_d(s) = \frac{-Z_c}{L_d(s)}\left[1+C_\pi s(Z_b+Z_{ed})+C_\mu sZ_b\right]$$

$$K_d(s) = \frac{1+C_\mu sZ_c}{L_d(s)}$$

$$Z'_e = Z_{ed}+Z_{ec}$$

$$L_c(s) \cong 1+g_m\left(Z'_e+\frac{Z_b}{\beta}\right)+C_\pi s(Z_b+Z'_e) +C_\mu s\left(Z_b+Z_c+(g_m+C_\pi s)\Delta_c\right)$$

and

$$\Delta_c = Z'_eZ_b+Z_bZ_c+Z'_eZ_c.$$

$K_d(s) = v_{\rm be}/v'_s$ is the transfer function from the input voltage v'_s to base–emitter voltage $v_{\rm be}$. $F_d(s) = 6V_t^3i_{c3}/(I_cv_{\rm be}^3)$ is the transfer function from $v_{\rm be}$ to the third-order collector current i_{c3}; the subscript of $F_d(s)_2$ in (3) implies that the operations are performed on the second-order current. $G(s) = v_{c3}/i_{c3}$ is the transfer function from the collector current to the output voltage; the subscript of $G_d(s)_3$ in (3) implies that the operations are performed on the third-order current. For a two-tone input signal, $V_s = v_1 + v_2$, $v_1 = A_1cos(\omega_1t)$, and $v_2 = A_2cos(\omega_2t)$, only second-order terms whose frequencies are $|\omega_2 - \omega_1|$ and $2\omega_2$ can generate intermodulation at frequency $2\omega_2-\omega_1$. Collecting all the intermodulation terms at frequency $2\omega_2 - \omega_1$, we have

$$\text{IM}_3 = \frac{\text{third-order output}}{\text{first-order output}} = \frac{I_{c0}}{96V_t^3}A_2^2\frac{\left|G_d\left(j(2\omega_2-\omega_1)\right)K_d(j\omega_2)^2K_d(j\omega_1)\right|}{|H_d(j\omega_1)|} \cdot\left|2F_d\left(j(\omega_2-\omega_1)\right)+F_d(2j\omega_2)\right|. \quad (4)$$

A lower third-order intermodulation (IM_3) is achieved when the last portion of (4) is minimized, while the first order is kept the same. By careful selection of Z_b, Z'_e, and Z_c, it is possible to make the last term in (4), i.e., $|2F_d(j(\omega_2-\omega_1))+F_d(j2\omega_2)|$, close to zero. However, the last terms are functions of $(\omega_2-\omega_1)$ and ω_2, and it is difficult to find a *general* solution for termination impedance to cancel the third-order nonlinearity. Another approach is to find the termination impedance such that $|F_d(j(\omega_2-\omega_1))|$ and $|F_d(2j\omega_2)|$ are separately close to zero. Such termination impedances are selected as

$$\begin{aligned} Z_b(j2\omega_2) &\cong 0\\ Z_b(j\Delta\omega) &\cong 0\\ Z'_e(j2\omega_2) &\cong \frac{1}{2g_m}\\ Z'_e(j\Delta\omega) &\cong \frac{1}{2g_m} \end{aligned} \quad (5)$$

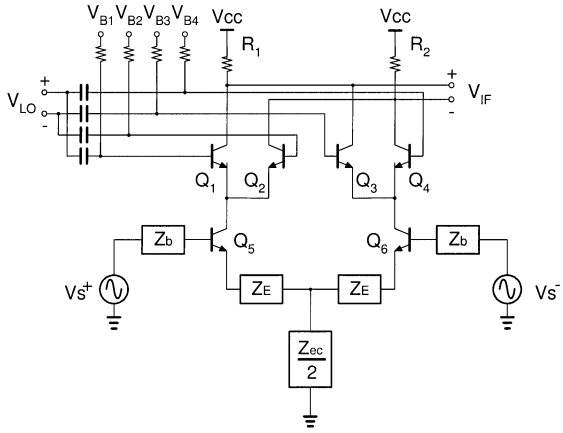

Fig. 3. Simplified model of bipolar double-balanced mixer.

where $\Delta\omega = |\omega_2-\omega_1|$. Substituting these value into $F_d(s)$, we obtain

$$\begin{aligned} |F_d(j\Delta\omega)| &\cong \frac{\Delta\omega|C_{je}-2\tau g_m|}{3g_m}\\ |F_d(2j\omega_2)| &\cong \frac{\frac{1}{g_m}\omega_2|C_{je}-2\tau g_m|}{\frac{3}{2}+\frac{C_\pi\omega_2}{g_m}}. \end{aligned} \quad (6)$$

For example, when $I_c = 2.5$ mA, with the setup and parameters used in [14], $|F_d(j\Delta\omega)| = 0.7$ and $|F_d(2j\omega_2)| = 0.37$ *without* the third-order cancellation termination, but $|F_d(j\Delta\omega)| = 0.007$ and $|F_d(2j\omega_2)| = 0.07$ *with* the third-order cancellation termination. It is clear that both $|F_d(j\Delta\omega)|$ and $|F_d(2j\omega_2)|$ can be decreased dramatically by the third-order termination cancellation.

III. Even-Order Distortion Analysis of the Double-Balanced Mixer

Fig. 3 shows a simplified model for the double-balanced bipolar mixer. Assuming the circuit input is symmetric, the output current of the transconductance $(Q_5 - Q_6)$ stage can be presented as the voltage-controlled current source. The *I–V* relation can be presented by

$$I_{c\_5} = I_{T5}+\gamma_1V_s^+ +\gamma_2V_s^{+2}+\gamma_3V_s^{+3} \quad (7a)$$

$$I_{c\_6} = I_{T6}+\gamma_1V_s^- +\gamma_2V_s^{-2}+\gamma_3V_s^{-3} \quad (7b)$$

where I_{T5} and I_{T6} are the dc-bias currents of Q_5 and Q_6, respectively. Generally, γ_1, γ_2, and γ_3 are not constant; they are functions of the frequencies of the input signals. Following the same nonlinear analysis as in Section II on the differential CE transconductance stage, the coefficients γ_1, γ_2, and γ_3 are derived as

$$\gamma_1 = \frac{C_\mu s\left[1+(g_m+C_\pi s)Z_{ed}\right]-g_m}{L_d(s)} \quad (8a)$$

$$\gamma_2 = g_{m2}\left(\frac{\left[1+C_\pi s(Z_b+Z'_e)+C_\mu sZ_b\right]}{L_c(s)}\right)_2\cdot K_d^2(s) \quad (8b)$$

$$\gamma_3 = g_{m3}\left(\frac{G_d(s)}{Z_c}\right)_3\left\{K_d(s)\cdot\left[F_d(s)_2K_d^2(s)\right]\right\}. \quad (8c)$$

The output currents contain even-order distortion terms; the most significant part is the second-order terms. The second-order currents of transistors Q_5 and Q_6 are

$$I_{c5\_2} = \gamma_{2\_5}\left(V_s^+\right)^2 \tag{9a}$$

$$I_{c6\_2} = \gamma_{2\_6}\left(V_s^-\right)^2. \tag{9b}$$

In an ideal double-balanced mixer, the second-order distortion currents I_{c5_2} and I_{c6_2} are equal and they are modulated by symmetric switching transistors $(Q_1 - Q_4)$. Since the second-order currents are divided equally in the switching transistors, there is no second-order voltage at the output. If the second-order currents are not equal or there are mismatches between switching transistors and between output resistors, the second-order currents will reach the output port. Based on a detailed analysis in the Appendix, the low-frequency second-order distortion output is

$$V_{\text{out}_2} \cong I_{c5\_2}\left(Rk_{12}\text{sech}^2\left(\frac{V_{\text{LO}}}{2V_T}\right) + \Delta\alpha_{12}R + \Delta R\right) + I_{c6\_2}\left(Rk_{34}\text{sech}^2\left(\frac{V_{\text{LO}}}{2V_T}\right) + \Delta\alpha_{34}R + \Delta R\right) \tag{10}$$

where

$$k_{12} = \frac{\Delta V_{B12} + V_T \ln\left(\dfrac{\alpha_2 I_{s1}}{\alpha_1 I_{s2}}\right)}{2V_T}$$

$$\Delta V_{B12} = V_{B1} - V_{B2}$$

$$\Delta\alpha_{12} = \frac{\alpha_1 - \alpha_2}{2}$$

$$R = \frac{R_1 + R_2}{2}$$

$$\Delta R = \frac{R_1 - R_2}{2}$$

I_{s1} and I_{s2} are saturation currents of transistors Q_1 and Q_2, and α_1 and α_2 are the common base current gains of transistors Q_1 and Q_2. ΔV_{B34}, k_{34}, and $\Delta\alpha_{34}$ are defined similarly.

Since the local oscillator (LO) signal is a periodic signal given by

$$V_{\text{LO}} = A_{\text{LO}}\cos(\omega_{\text{LO}}t) \tag{11}$$

the mismatch transfer function term $\text{sech}^2(V_{\text{LO}}/2V_T)$ can be expanded as

$$\text{sech}^2\left(\frac{V_{\text{LO}}}{2V_T}\right) = B_0(A_{\text{LO}}) + B_2(A_{\text{LO}})\cdot\cos(2\omega_{\text{LO}}t) + B_4(A_{\text{LO}}) \cdot\cos(4\omega_{\text{LO}}t) + B_6(A_{\text{LO}})\cdot\cos(6\omega_{\text{LO}}t)\cdots. \tag{12}$$

The Fourier coefficients of the mismatch transfer function $\text{sech}^2(V_{\text{LO}}/2V_T)$ are show in Fig. 4 and they are functions of the LO amplitude A_{LO}. In these coefficients, B_0 is the most important because it makes the low-frequency envelope distortion of the input signal appear at the output port. The $B_2(A_{\text{LO}})\cdot\cos(2\omega_{\text{LO}}t)$ term transfers the second-order signal at frequency $(\omega_1+\omega_2)$ to frequency $|\omega_1+\omega_2-2\omega_{\text{LO}}|$, which is mostly out of the baseband and is, therefore, negligible. Substituting (12) into (10) and neglecting the insignificant terms, the second-order output is

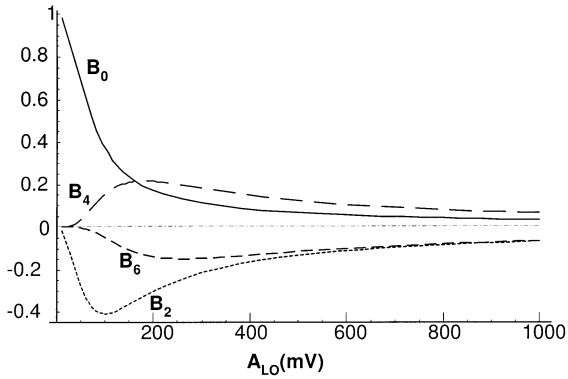

Fig. 4. Fourier-transform coefficients of the mismatch transfer function $\text{sech}^2(V_{\text{LO}}/2V_T)$. B_0 is the primary component affecting IIP_2.

$$V_{\text{out}_2} = I_{c5\_2}(R\,k_{12}B_0 + \Delta\alpha_{12}R + \Delta R) + I_{c6\_2}(R\,k_{34}B_0 + \Delta\alpha_{34}R + \Delta R). \tag{13}$$

Since B_0 is a function of the LO amplitude, the second-order nonlinearity is also a function of the LO amplitude, which was observed previously in [10]. As a result, a stable amplitude of the LO signal is required for excellent second-order nonlinearity cancellation. Since the mismatches between transistors Q_5 and Q_6, the mismatches between termination impedances of each transistor and the mismatches between inputs V_s^+ and V_s^- can mismatch the second-order currents I_{c5_2} and I_{c6_2}, and since k_{12} is generally not equal to k_{34}, tuning R_1 and R_2 alone cannot cancel the second-order distortion effectively. Instead of tuning the output resistor R_1 and R_2, the mismatch factor k_{12} and k_{34} can be tuned separately by tuning the dc-bias voltages of the mixer. From (13), if

$$R\,k_{12}B_0 + \Delta\alpha_{12}R + \Delta R = 0 \tag{14a}$$

$$R\,k_{34}B_0 + \Delta\alpha_{34}R + \Delta R = 0 \tag{14b}$$

then the second-order nonlinearity terms due to mismatches of the mixer are cancelled. Solving (14) to eliminate second-order distortion, we have

$$\Delta V_{B12} = -2V_T\left(\frac{1}{B_0}\left(\Delta\alpha_{12} + \frac{\Delta R}{R}\right) + \frac{1}{2}\ln\sqrt{\frac{\alpha_2 I_{s1}}{\alpha_1 I_{s2}}}\right) \tag{15a}$$

$$\Delta V_{B34} = -2V_T\left(\frac{1}{B_0}\left(\Delta\alpha_{34} + \frac{\Delta R}{R}\right) + \frac{1}{2}\ln\sqrt{\frac{\alpha_4 I_{s3}}{\alpha_3 I_{s4}}}\right). \tag{15b}$$

As a result, by separately tuning the bias of the double-balanced mixer, the envelope distortion caused by even-order nonlinearity and mismatches can be drastically reduced. The other benefit from this scheme is that it is much easier to tune the bias voltages than to tune the resistors on an integrated circuit (IC).

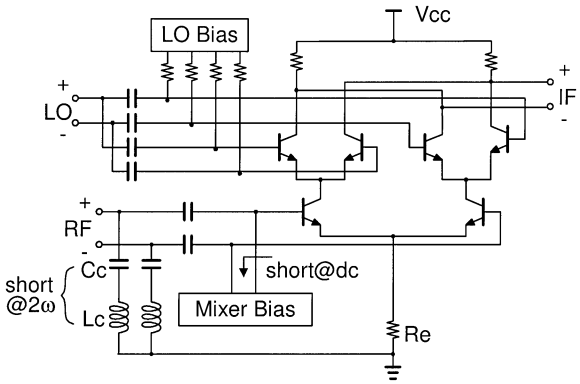

Fig. 5. Down-conversion double-balanced active mixer with third-order cancellation.

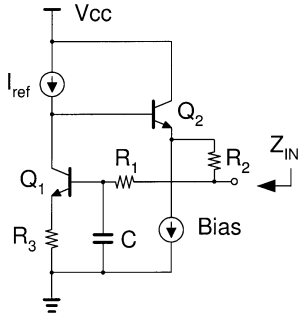

Fig. 6. Mixer bias circuit to provide low impedance at dc.

IV. Low Third-Order Distortion Double-Balanced Mixer Design

The termination condition in (5) suggests that only the second-order currents need to be terminated at the input and Z_e' needs to be real at the second harmonic of the input signals. By connecting two emitters of the differential pair and letting $R_e = 1/g_m - 2\,r_e$, the emitter impedance requirement for third-order cancellation can be easily satisfied. The resistor is only added for common-mode operation so the noise is not increased for the differential circuit, as was pointed out in [5]. Fig. 5 shows a simplified down-conversion mixer. The second-order base termination at frequency 2ω is achieved through series resonance components L_c and C_c. The base termination at frequency $\Delta\omega$ was achieved with the feedback circuit of Fig. 6. The impedance of the bias circuit at dc and RF frequency are

$$Z_{\text{in}}(dc) \cong \frac{R_3}{\beta_2} + \frac{R_2}{g_{m_1} r_{o1}} \left(1 + \frac{R_1 g_{m_1}}{\beta_1}\right) \tag{16a}$$

$$Z_{\text{in}}(\omega) \cong R_2 // R_1. \tag{16b}$$

If L_c and C_c are ideal, they do not add noise to the circuit; they only change the optimum source impedance matching. However, the real inductor does add some noise to the circuit due to its finite series resistance. We will analyze the effect of the base termination impedance at 2ω with the classic two-port model. The noise model is shown in Fig. 7. The noise i_p generated by the series resistance of L_c is uncorrelated with other noise sources as follows:

$$\overline{i_p^2} = 4kT\Delta f R_{lc} \left|Y_p^2\right| \tag{17}$$

where R_{lc} is the series resistance of the inductor L_c and Y_p is the admittance of the second-order termination. The noise factor of the system *without* second-order harmonic termination is given by the well-known expression [15]

$$F = \frac{\overline{i_s^2} + \overline{|i_u + (Y_c + Y_s)e_n|^2}}{\overline{i_s^2}} = 1 + \frac{G_u + \left[(G_c + G_s)^2 + (B_c + B_s)^2\right] R_n}{G_s} \tag{18}$$

where

$$\begin{aligned} i_n &= i_c + i_u \\ i_c &= Y_c e_n \\ R_n &\equiv \frac{\overline{e_n^2}}{4kT\Delta f} \\ G_u &\equiv \frac{\overline{i_u^2}}{4kT\Delta f} \\ G_s &\equiv \frac{\overline{i_s^2}}{4kT\Delta f} \\ Y_c &= G_c + jB_c \\ Y_s &= G_s + jB_s. \end{aligned}$$

The conductance of the second harmonic termination increases the current noise at the input, and it changes the overall impedance seen by the two-port network. The total effective conductance of the second harmonic termination and the input source is

$$Y_s' = Y_s + Y_p. \tag{19}$$

Thus, the noise factor of the system *with* second harmonic termination is

$$F' = \frac{\overline{i_s^2} + \overline{i_p^2} + \overline{|i_u + (Y_c + Y_s')e_n|^2}}{\overline{i_s^2}} = 1 + \frac{G_p + G_u}{G_s} + \frac{\left[(G_c + G_s')^2 + (B_c + B_s')^2\right] R_n}{G_s} \tag{20}$$

where

$$\begin{aligned} G_p &\equiv \frac{\overline{i_p^2}}{4kT\Delta f} \cong \frac{1}{9QL_c\omega_{\text{rf}}} \\ \omega_{\text{rf}} &= \sqrt{\frac{1}{4C_cL_c}} \\ Q &= \frac{\omega_{\text{rf}} L_c}{R_{lc}} \\ Y_p' &= G_p' + jB_p'. \end{aligned} \tag{21}$$

Comparing (18) and (20), the difference is the extra noise term G_p, as well as G_s' and B_s' are in the equation instead of G_s and B_s due to the second harmonic termination. It is well known that when G_s is

$$G_{\text{opt}} = \sqrt{\frac{G_u}{R_n} + G_c^2} \tag{22a}$$

and

$$B_s = -B_c \tag{22b}$$

the noise factor has a minimum value

$$F_{\min} = 1 + 2R_n(G_{\text{opt}} + G_c). \tag{23}$$

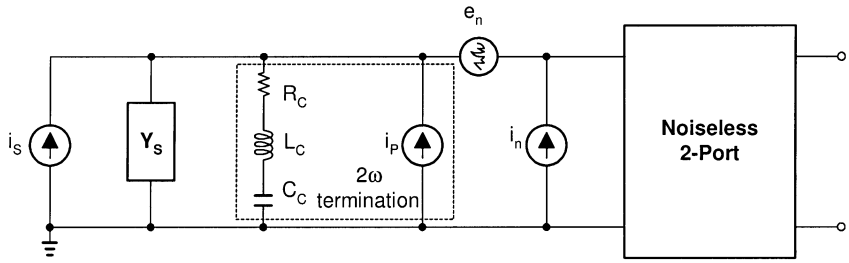

Fig. 7. Equivalent two-port noise model of mixer showing the effect of 2ω termination.

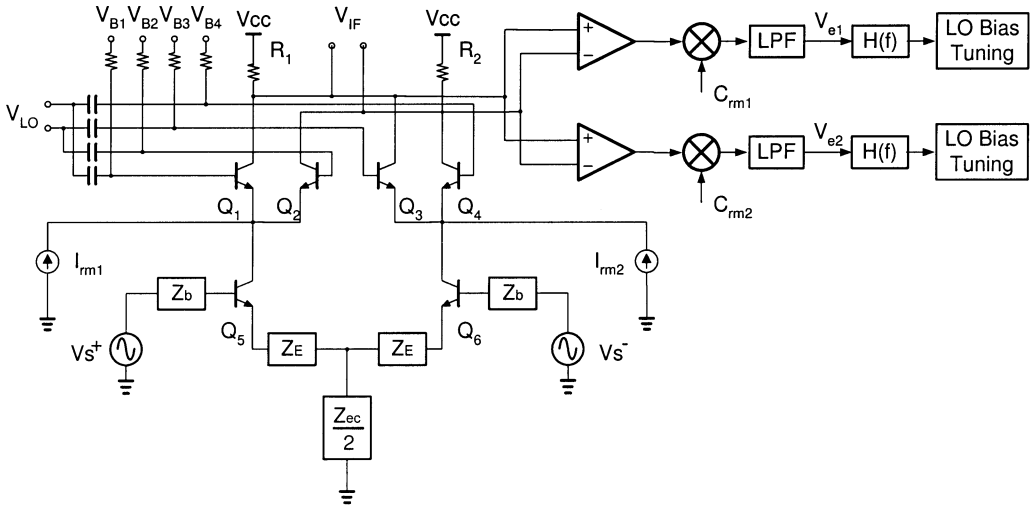

Fig. 8. Proposed even-order distortion cancellation scheme of the double-balanced mixer.

Due to the second harmonic termination, the optimum G_s is changed to

$$G'_{\rm opt} = \sqrt{\frac{G_u + G_p}{R_n} + (G_c + G_p)^2} \tag{24a}$$

and

$$B_s = -B_c - B_p. \tag{24b}$$

With the second harmonic termination, the minimum noise factor is

$$F'_{\rm min} = 1 + 2R_n\Big(G'_{\rm opt} + G_c + G_p\Big). \tag{25}$$

The minimum noise factor increases by

$$\Delta F = F'_{\rm min} - F_{\rm min} = 2R_n\Big(G'_{\rm opt} - G_{\rm opt} + G_p\Big). \tag{26}$$

From (21), if G_p is selected to be much smaller than G_u and G_c, the increase of the minimum noise factor is small. For example, if $Q = 10$, $L_c = 6$ nH, and $\omega_{\rm rf} = 2.15$ GHz, G_p is equivalent to the conductance of a 7.3-kΩ resistor. This resistance is usually much larger than the optimum noise matching impedance of a well-designed CE stage. As a result, the noise increase is negligible.

V. Even-Order Distortion Cancellation Scheme of the Double-Balanced Mixer

In order to cancel the second-order distortion, a mismatch detection and cancellation scheme is proposed. Fig. 8 is a block diagram for the second-order distortion cancellation scheme. A pair of pseudorandom (PN) currents are injected at two pairs of the emitters of the switching transistors, and they are represented by

$$I_{\rm rm1} = I_a C_{\rm rm1} \tag{27a}$$

$$I_{\rm rm2} = I_a C_{\rm rm2} \tag{27b}$$

where I_a is the current amplitude of the PN currents, $C_{\rm rm1}$ and $C_{\rm rm2}$ are two uncorrelated PN sequences. Due to the mismatches of the double-balanced mixer, the PN signals appear at the output of the mixer. Assuming the high-frequency signals at double LO frequency are filtered out, the low-frequency output part containing the PN signals is

$$V_{\rm out\_rm} = I_{\rm rm1}(R\,k_{12}B_0 + \Delta\alpha_{12}R + \Delta R) + I_{\rm rm2}(R\,k_{34}B_0 + \Delta\alpha_{34}R + \Delta R). \tag{28}$$

At the output of the mixer, the output voltage is correlated with the PN codes $C_{\rm rm1}$ and $C_{\rm rm2}$. Assuming the PN sequences are uncorrelated with the desired signal and noise, the mismatch error voltages at the output are

$$V_{e1} = I_a(R\,k_{12}B_0 + \Delta\alpha_{12}R + \Delta R) \tag{29a}$$

$$V_{e2} = I_a(R\,k_{34}B_0 + \Delta\alpha_{34}R + \Delta R). \tag{29b}$$

The mismatch error voltages are processed by following loop filter $H(s)$, the output voltage are then used to tune the LO dc-bias voltage. In the s domain, the outputs of the loop filters are

$$\Delta V_{B12}(s) = V_{e1}(s) \cdot H(s) \tag{30a}$$

$$\Delta V_{B34}(s) = V_{e2}(s) \cdot H(s). \tag{30b}$$

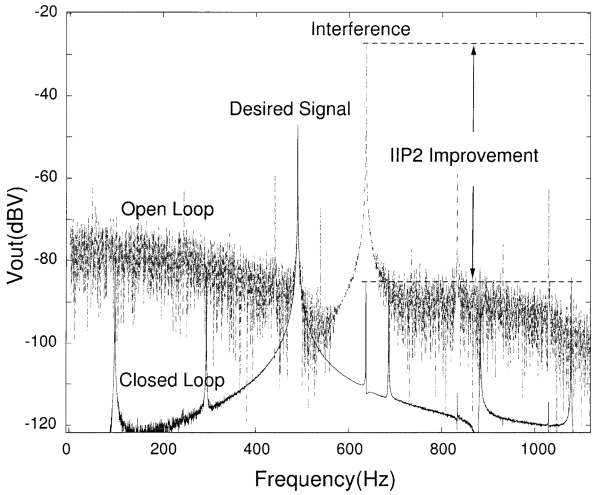

Fig. 9. Simulated closed-loop second-order nonlinearity cancellation result.

Substituting k_{12}, k_{34}, and (29) into (30), the dc-bias voltage are solved to be

$$\Delta V_{B12}(s) = \frac{I_a R B_0 \ln\dfrac{\alpha_2 I_{s1}}{\alpha_1 I_{s2}}}{2} + I_a \Delta\alpha_{12} R + I_a \Delta R \over 1 - \dfrac{I_a R B_0}{2V_T} H(s) H(s) \quad (31a)$$

$$\Delta V_{B34}(s) = \frac{I_a R B_0 \ln\dfrac{\alpha_4 I_{s3}}{\alpha_3 I_{s4}}}{2} + I_a \Delta\alpha_{34} R + I_a \Delta R \over 1 - \dfrac{I_a R B_0}{2V_T} H(s) H(s). \quad (31b)$$

By choosing a simple loop filter as an integrator $H(s) = -1/s$, the dc-bias voltage are found to be exactly the solution described in (15). Fig. 9 is a simulation result of the closed-loop second-order nonlinearity cancellation. In this simulation, a relatively large low-frequency current at frequency 650 Hz is injected from the switching transistor input to simulate the second-order distortion of a strong interfering signal, two independent random binary signals with date rate of 300 bit/s are injected along with the interfering signal, the desired output is at frequency 500 Hz. The initial ΔV_{B12} and ΔV_{B34} are 5 mV, switching transistor mismatch is set to 5%, $\Delta R/R$ is 1% and $\Delta\alpha$ is 3%. After the initial response of the close loop settled, the final ΔV_{B12} and ΔV_{B34} are changed to -22 mV. The second-order interference is decreased by 60 dB and the desired signal is not changed; thus, IIP_2 is increased by 60 dB in this simulated case. The random signals injected at the emitter of the switching transistors add noise to the desired signal, but this noise is cancelled along with the interference signal and add little noise when the loop settles.

VI. Measurement Results

The mixer was fabricated in IBM's SiGe5AM process with transistor peak $f_T \cong 45$ GHz. The microphotograph of the mixer is shown in Fig. 10. The mixer has been characterized at 2.1 GHz.

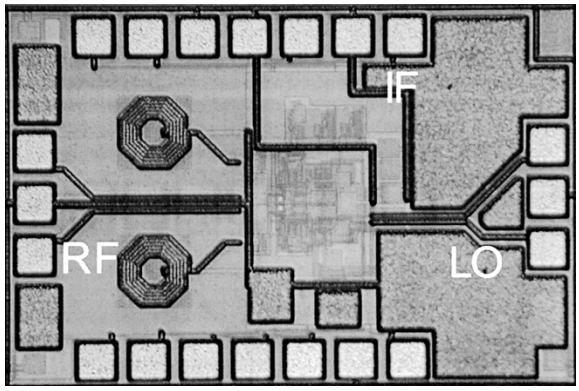

Fig. 10. Microphotograph of the SiGe HBT WCDMA mixer.

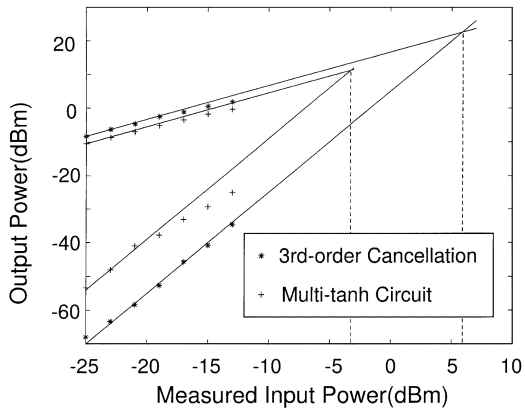

Fig. 11. Measured third-order intermodulation characteristics. $I_{\mathrm{dc}} = 2.2$ mA for third-order cancellation circuit and 3 mA for *multitanh* circuit.

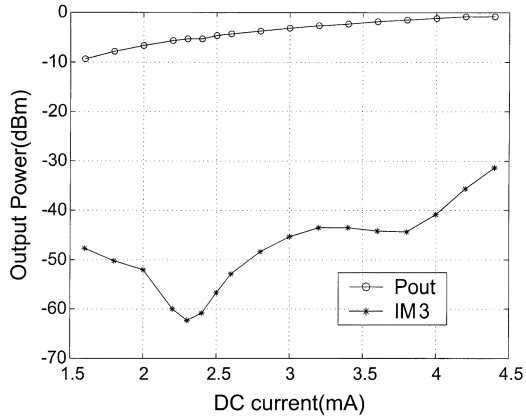

Fig. 12. Measured third-order intermodulation versus dc-bias current. $P_{\mathrm{in}} = -22$ dBm.

The output power as well as the third-order intermodulation are plotted in Fig. 11. The mixer is operated from a 2.7-V dc supply and consumes approximately 2.2-mA current. The mixer with the third-order nonlinearity cancellation is compared with a mixer with a *multitanh* input stage, which is similar to the input stage used in [17]. Both circuits are fabricated on the same wafer, the difference between the two mixers are the input stages. The multitanh circuit is not terminated with the second-order harmonic termination, and the bias currents are set with current sources. The mixer with a multitanh input stage is also operated from 2.7-V dc supply, but it is biased at 3-mA dc current. The mixer with the third-order nonlinearity cancellation

TABLE I
COMPARISON WITH OTHER RECENT MIXERS

Ref.	F_{RF} (GHz)	Gain (dB)	NF (dB)	IIP3 (dBm)	P_{diss} (mW)	Process	FOM (dB)
This work	2.15	15.8	7.2	6.0	5.9	0.5μSiGe BiCMOS	22.2
[19]	0.88	8.4	7.6 SSB	8.0	12.0	0.5μSiGe BiCMOS	23.4
[20]	2.0	15.0	8.5	-1.5	9.1	$0.35\mu m$ BiCMOS	11.6
[21]	1.9	6.1	10.9 SSB	2.3	4.75	$0.8\mu m$ SiBJT	18.0
[18]	2.0	24.2	3.2	-1.5	21.6	$0.35um$ CMOS	14.8

has superior performance; it has higher gain with lower power consumption. The linearity of the mixer with the third-order nonlinearity cancellation is also approximately 10 dB better.

Fig. 12 is a plot of nonlinearity characteristic versus dc-bias current of the mixer at an input power of -22 dBm and an LO power of 0 dBm. Table I is a summary of the mixer, as well as a comparison with other recent mixers. The figure-of-merit is defined in [18] as

$$\mathrm{FOM} = 10\log\left(\frac{\mathrm{IIP3(mW)}}{(F-1)\cdot V_{dd}\cdot I_{\mathrm{dc}}}\right). \tag{32}$$

The results generally exceed the performance of the other previously reported results. The mixer in [19] has similar performance, but is operated at 880 MHz.

The mixer is also measured for the second-order nonlinearity performance. The mixer bias is set by the resistor network on the IC, but they can be tuned with a variable resistor from the outside. The mixer has an IIP_2 of 19 dBm without the tuning of the bias; its IIP_2 increased to 49 dBm when the bias tuning circuit is connected. As a result, the IIP_2 of the mixer is improved by approximately 30 dB by the second-order cancellation technique.

VII. CONCLUSION

The general nonlinear responses of the CE differential-pair circuit have been developed to determine the conditions for cancellation of third-order nonlinearities; the second-order nonlinear response of the bipolar double-balanced mixer is also analyzed to determine the conditions for cancellation of the envelope distortion. A WCDMA down-conversion mixer has been designed using these techniques. The designed mixer exhibits state-of-the-art linearity at very low dc power without excessive penalty on noise figure.

APPENDIX
DERIVATION OF THE MISMATCH EFFECTS ON SECOND-ORDER DISTORTION OF THE DOUBLE-BALANCED BIPOLAR MIXER

As shown in Fig. 3, the emitter currents of transistor Q_1 and Q_2 are

$$I_{e1} = \frac{I_{s1}}{\alpha_1} e^{\frac{V_{B1}+\frac{V_{\mathrm{LO}}}{2}-V_{c5}}{V_t}} \tag{33a}$$

$$I_{e2} = \frac{I_{s2}}{\alpha_2} e^{\frac{V_{B2}-\frac{V_{\mathrm{LO}}}{2}-V_{c5}}{V_t}} \tag{33b}$$

$$I_{c5} = I_{e1} + I_{e2} \tag{33c}$$

where V_{B1} and V_{B2} are the dc-bias voltages of transistors Q_1 and Q_2

$$\alpha_1 = \frac{\beta_1}{\beta_1+1}$$
$$\alpha_2 = \frac{\beta_2}{\beta_2+1}.$$

Solving (33), the emitter current difference between transistor Q_1 and Q_2 is

$$\Delta I_{e12} = I_{e1} - I_{e2} \cong I_{c5}\tanh\left(\overbrace{\frac{V_{\mathrm{LO}}}{2V_T}}^{\text{ideal}} + \frac{\overbrace{V_{B1}-V_{B2}+V_T\ln\left(\frac{\alpha_2 I_{s1}}{\alpha_1 I_{s2}}\right)}^{\text{mismatch effects}}}{2V_T}\right). \tag{34}$$

Considering the β mismatch of Q_1 and Q_2, the output currents are

$$\begin{aligned}\Delta I_{c12} &= I_{c1} - I_{c2}\\ &= \alpha_1 I_{e1} - \alpha_2 I_{e2}\\ &= \alpha_{12}(I_{e1}-I_{e2}) + \Delta\alpha_{12} I_{c5} \qquad (35a)\\ I_{c12} &= I_{c1} + I_{c2}\\ &= \Delta\alpha_{12}(I_{e1}-I_{e2}) + \alpha_{12} I_{c5} \qquad (35b)\end{aligned}$$

where

$$\alpha_{12} = \frac{\alpha_1+\alpha_2}{2}$$
$$\Delta\alpha_{12} = \frac{\alpha_1-\alpha_2}{2}.$$

Substituting (34) into (35), the output current is

$$\Delta I_{c12} = I_{c5}\left(\alpha_{12}\tanh\left(\frac{V_{\mathrm{LO}}}{2V_T}+k_{12}\right)+\Delta\alpha_{12}\right) \tag{36}$$

where

$$k_{12} = \frac{\Delta V_{B12} + V_T\ln\left(\frac{\alpha_2 I_{s1}}{\alpha_1 I_{s2}}\right)}{2V_T}.$$

k_{12} is the mismatch factor of transistor Q_1 and Q_2; it is a function of the dc-bias voltage mismatch $\Delta V_{B12} = V_{B1} - V_{B2}$,

the transistor saturation current mismatch I_{s1}/I_{s2}, and the transistor β mismatch α_1/α_2. Assuming k_{12} is small compared to $V_{\rm LO}/2V_T$, (36) can be expanded as

$$\Delta I_{c12} = \overbrace{I_{c5}\alpha_{12}\tanh\left(\frac{V_{\rm LO}}{2V_T}\right)}^{\text{ideal}} + \overbrace{I_{c5}\left(k_{12}\text{sech}^2\left(\frac{V_{\rm LO}}{2V_T}\right)+\Delta\alpha_{12}\right)}^{\text{mismatch effects}}. \quad (37)$$

The driving LO signal on Q_3 and Q_4 has an opposite sign with the LO signal on Q_1 and Q_2 so the output current ΔI_{c34} is

$$\Delta I_{c34} = -I_{c6}\alpha_{34}\tanh\left(\frac{V_{\rm LO}}{2V_T}\right) + I_{c6}\left(k_{34}\text{sech}^2\left(\frac{V_{\rm LO}}{2V_T}\right)+\Delta\alpha_{34}\right). \quad (38)$$

The output voltage is

$$\begin{aligned} V_{\rm out} &= R_1(I_{c1}+I_{c3}) - R_2(I_{c2}+I_{c4}) \\ &= R(\Delta I_{c12}+\Delta I_{c34}) + \Delta R(I_{c12}+I_{c34}) \\ &\cong R(\alpha_{12}\Delta I_{e12} + \Delta\alpha_{12}I_{c5} + \alpha_{34}\Delta I_{e34} + \Delta\alpha_{34}I_{c6}) \\ &\quad + \Delta R(\alpha_{12}I_{c5}+\alpha_{34}I_{c6}) \end{aligned} \quad (39)$$

where

$$R_1 = R + \Delta R$$
$$R_2 = R - \Delta R.$$

Substituting (34), (36), and (38) into (39), the output voltage is

$$\begin{aligned} V_{\rm out} &= R\tanh\left(\frac{V_{\rm LO}}{2V_T}\right)(\alpha_{12}I_{c5}-\alpha_{34}I_{c6}) \\ &\quad + I_{c5}\left(R\alpha_{12}k_{12}\text{sech}^2\left(\frac{V_{\rm LO}}{2V_T}\right)+\Delta\alpha_{12}R+\Delta R\alpha_{12}\right) \\ &\quad + I_{c6}\left(R\alpha_{34}k_{34}\text{sech}^2\left(\frac{V_{\rm LO}}{2V_T}\right)+\Delta\alpha_{34}R+\Delta R\alpha_{34}\right) \\ &\cong R\tanh\left(\frac{V_{\rm LO}}{2V_T}\right)(I_{c5}-I_{c6}) \\ &\quad + I_{c5}\left(Rk_{12}\text{sech}^2\left(\frac{V_{\rm LO}}{2V_T}\right)+\Delta\alpha_{12}R+\Delta R\right) \\ &\quad + I_{c6}\left(Rk_{34}\text{sech}^2\left(\frac{V_{\rm LO}}{2V_T}\right)+\Delta\alpha_{34}R+\Delta R\right). \end{aligned} \quad (40)$$

The conditions $\alpha_{12}\cong 1$ and $\alpha_{34}\cong 1$ are used in (40).

ACKNOWLEDGMENT

The authors would like to acknowledge many valuable discussions with Prof. P. Asbeck and Prof. I. Galton, both of the University of California at San Diego (UCSD), La Jolla, V. Aparin, Qualcomm, San Diego, CA, and Prof. L. de Vreede, Technical University of Delft, Delft, The Netherlands.

REFERENCES

[1] O. K. Jensen, T. E. Kolding, C. R. Iversen, S. Laursen, R. V. Reynisson, J. H. Mikkelsen, E. Pedersen, M. B. Jenner, and T. Larsen, "RF receiver requirements for 3G W-CDMA mobile equipment," *Microwave J.*, vol. 43, no. 2, pp. 22–46, Feb. 2000.

[2] L. E. Larson, *RF and Microwave Circuit Design for Wireless Communications*. Norwood, MA: Artech House, 1996.

[3] V. Aparin and C. Persico, "Effect of out-of-band terminations on intermodulation distortion in common-emitter circuits," in *IEEE MTT-S Int. Microwave Symp. Dig.*, 1999, pp. 977–980.

[4] K. Fong and R. G. Meyer, "High-frequency nonlinearity analysis of common-emitter and differential-pair transconductance stages," *IEEE J. Solid-State Circuits*, vol. 33, pp. 548–555, Apr. 1999.

[5] M. Heijden, H. Graaff, and L. Vreede, "A novel frequency-independent third-order intermodulation distortion cancellation technique for BJT amplifiers," *IEEE J. Solid-State Circuits*, vol. 37, pp. 1176–1183, Sept. 2002.

[6] B. Razavi, "Challenges and trends in RF design," in *9th Annu. IEEE Int. ASIC Conf. and Exhibit.*, 1996, pp. 81–86.

[7] A. A. Abidi, "Direct-conversion radio transceivers for digital communications," *IEEE J. Solid-State Circuits*, vol. 30, pp. 1399–1410, Dec. 1995.

[8] E. E.Edwin E. Bautista, B.Babak Bastani, and J.Joseph Heck, "A high IIP2 downconversion mixer using dynamic matching," *IEEE J. Solid-State Circuits*, vol. 35, pp. 1934–1941, Dec. 2000.

[9] T. Yamaji and H. Tanimoto *et al.*, "An I/Q active balanced harmonic mixer with IM2 cancelers and a 45 degrees phase shifter," *IEEE J. Solid-State Circuits*, vol. 33, pp. 2240–2246, Dec. 1998.

[10] K. Kivekäs, A. Pärssinen, and K. A. I. Halonen, "Characterization of IIP2 and DC-offset in transconductance mixers," *IEEE Trans. Circuits Syst. II*, vol. 48, pp. 1028–1038, Nov. 2001.

[11] K. Kivekäs, A. Pärssinen, J. Ryynänen, J. Jussila, and K. A. I. Halonen, "Calibration techniques of active BiCMOS mixers," *IEEE J. Solid-State Circuits*, vol. 37, pp. 594–602, June 2002.

[12] J. Ryynänen, K. Kivekäs, J. Jussila, L. Sumanen, A. Pärssinen, and K. A. I. Halonen, "A single-chip multimode receiver for GSM900, DCS1800, PCS1900, and WCDMA," *IEEE J. Solid-State Circuits*, vol. 38, pp. 594–602, Apr. 2003.

[13] S. A. Maas, *Nonlinear Microwave Circuits*. Piscataway, NJ: IEEE Press, 1997.

[14] L. Sheng and L. E. Larson, "A general theory of third-order intermodulation distortion in common-emitter radio frequency," in *Proc. Int. Circuits and Systems Symp.*, vol. 1, May 2003, pp. 177–180.

[15] T. H. Lee, *The Design of CMOS Radio-Frequency Integrated Circuits*. Cambridge, U.K.: Cambridge Univ. Press, 1998.

[16] P. Wambacq and W. Sansen, *Distortion Analysis of Analog Integrated Circuits*. Norwell, MA: Kluwer, 1993.

[17] L. Sheng, J. Jensen, and L. E. Larson, "A wide-bandwidth Si/SiGE HBT direct conversion sub-harmonic mixer/downconverter," *IEEE J. Solid-State Circuits*, vol. 35, pp. 1329–1337, Sept. 2000.

[18] A. Karimi-Sanjaani, H. Sjoland, and A. A. Abidi, "A 2 GHz merged CMOS LNA and mixer for WCDMA," in *VLSI Circuits Tech. Symp. Dig.*, 2001, pp. 19–22.

[19] V. Aparin, E. Zeisel, and P. Gazzerro, "Highly linear SiGe BiCMOS LNA and mixer for cellular CDMA/AMPS applications," in *IEEE Radio Frequency Integrated Circuits Symp.*, 2002, pp. 129–132.

[20] K. Kivekäs, A. Pärssinen, J. Jussila, J. Ryynänen, and K. Halonen, "Design of low-voltage active mixer for direct conversion receivers," in *IEEE Int. Circuits and Systems Symp.*, vol. 4, 2001, pp. 382–385.

[21] J. R. Long and M. A. Copeland, "A 1.9 GHz low-voltage silicon bipolar receiver front-end for wireless personal communications system," *IEEE J. Solid-State Circuits*, vol. 30, pp. 1438–1448, Dec. 1995.

Liwei Sheng was born in Liaoning, China, in 1971. He received the B.S. and M.S. degrees in electrical engineering from Peking University, Beijing, China, in 1994 and 1997 respectively, and is currently working toward the Ph.D. degree at the University of California at San Diego, La Jolla.

His research concerns high-frequency ICs for wireless communications.

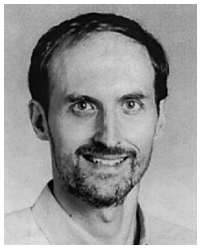

Lawrence E. Larson (S'82–M'86–SM'90–F'00) received the B.S. and M. Eng. degrees in electrical engineering from Cornell University, Ithaca, NY, in 1979 and 1980, respectively, and the Ph.D. degree in electrical engineering and MBA degree from the University of California at Los Angeles (UCLA), in 1986 and 1996, respectively.

From 1980 to 1996, he was with Hughes Research Laboratories, Malibu, CA, where he directed the development of high-frequency microelectronics in GaAs, InP, and Si–SiGe and microelectromechanical system (MEMS) technologies. In 1996, he joined the faculty of the University of California at San Diego (UCSD), La Jolla, where he is currently the Inaugural Holder of the Communications Industry Chair. He is currently Director of the UCSD Center for Wireless Communications. During the 2000–2001 academic year, he was on leave with IBM Research, San Diego, CA, where he directed the development of RF integrated circuits (RFICs) for third-generation (3G) applications. He has authored or coauthored over 150 papers and has coauthored three books. He holds 25 U.S. patents.

Dr. Larson was the recipient of the 1995 Hughes Electronics Sector Patent Award for his work on RF MEMS technology. He was corecipient of the 1996 Lawrence A. Hyland Patent Award of Hughes Electronics for his work on low-noise millimeter-wave high electron-mobility transistors (HEMTs), and the 1999 IBM Microelectronics Excellence Award for his work in Si–SiGe HBT technology.